AIAA-94-0511

Numerical Analysis Concepts for Balloon Analysis

W. Anderson, J. park and M. Dungan
Univ of Michigan
Ann Arbor, MI

32nd Aerospace Sciences Meeting & Exhibit
January 10-13, 1994 / Reno, NV

AIAA-94-0511

Numerical Analysis Concepts for Balloon Analysis

W. J. Anderson,* Jungsun Park † and Michael Dungan ‡
Dept. of Aerospace Engineering, Univ. of Michigan, Ann Arbor MI 48109.

Abstract

Structural, thermal and acoustic numerical analysis concepts are reviewed in regard to their suitability for high-altitude balloon analysis. Finite element theory is the main tool for structural analysis, yet the solution process in the commercial codes is not satisfactory in all ways. Comparisons are made between theory and commercial codes in the analysis of thin balloon structures. MARC, ABAQUS and MSC/NASTRAN are compared with a series solution of the membrane differential equation. The structural problem is treated as a small strain, large-displacement type.

The thermal problem for the high-altitude balloon deserves treatment with modern CFD codes. New finite element fluid codes show promise for the internal buoyant convection in the balloons caused by solar heating. An axisymmetric solution is shown for the 22 million cubic foot balloon.

A balloon in flight displaces an amount of air which is approximately equal to the balloon's weight. When the balloon accelerates, some of the surrounding air must also accelerate with the balloon, creating "added" mass, which must be properly predicted. Acoustic codes are able to find the added mass of a balloon, which is modeled as a rigid body immersed in an inviscid, incompressible fluid (air). The effect of mesh size is investigated. The results agree moderately well with the only experiment at hand.

Nomenclature

E	= Young's modulus
h	= thickness of membrane
[K]	= stiffness matrix
L	= characteristic plan dimension
N_r,N_t	= membrane force component/unit length
R^2	= goodness of curve fit
y(x)	= polynomial fit for inertia coefficient
ν	= Poisson's ratio
ρ	= fluid density

Introduction

It is important to accurately model the structure of the high altitude balloon to predict failure and to optimize the design. Thermal studies are important to predict the interior temperature field, since this characterizes the lift provided by the helium.

High altitude balloons are very large and made of very thin polyethylene film. The thickness of 0.015 mm (0.0006 in) means that the balloon should be modeled structurally with good membrane elements. The commercial FEA programs do have membrane elements, but the solution often diverges if at the first load step the membrane is untensioned. The slack membrane has no lateral stiffness and leads to a singular solution. Also, as the solution proceeds, wrinkles are created and disappear, and the FEA program has trouble following the rapid changes. Divergence of the nonlinear solution is often the result.

Commercial computer programs are studied in each of three areas: structural response, thermal response and added mass. When available, alternate codes are compared.

Structural Analysis

It is important to simulate the pneumatic inflation of membrane in the cases of high-altitude balloons, automobile safety air bags and aircraft emergency escape

*Professor of Aerospace Engineering, Senior Member AIAA.
†Visiting Scientist, Aerospace Engineering.
‡Graduate Student, Aerospace Engineering.

slides (which double as life rafts). Each is a thin, membrane material which has a tendency to wrinkle and fold as it is inflated, causing multiple contacts between surfaces. The mood of the analyst is generally one of despair when attempting to solve the full problem of inflation of a general membrane structure. The bookkeeping of the multiple contact surfaces is too severe, even for commercial codes that have strong contact capability. MARC and ABAQUS, for instance, cannot currently handle the wealth of contacts possible in say, a square meter of polyethlyene film crushed in a fist.

Let us consider a lesser problem, the "start-up" problem for the lateral deflection of a flat membrane. We will create a standard problem: a circular disk 4 m in diameter, clamped at the edges, made of 0.015 mm thick isotropic polyethylene film, with Young's modulus of 600 MPa and Poisson's ratio of 0.3. The lateral pressure on the initially flat, unstressed disk ranges from 10^{-8} MPa to $5.\times10^{-6}$ MPa. The deflection is strongly nonlinear and the system is a stiffening type. The problem is characterized by small strain and large deflection. A theoretical analysis of such a circular disk is given in the Appendix, using a series solution of the differential equation of equilibrium.

The "start-up" problem for initially unstressed membranes is difficult because they have no lateral stiffness. (This can be alleviated by initial curvature or initial tension.) Commercial computer codes MSC/NASTRAN, MARC and ABAQUS have trouble in starting the inflation solution, typically diverging at the first load step. The lateral load is unopposed by any lateral stiffness, and an enormous displacement results. There are displacement-control methods available (Riks method and modified Riks method) which can avoid problems which occur during a solution, once underway, but don't seem to help at start-up.

Several "work-arounds" are candidates for taming the start-up problem:

Fading thermal stress One can impose a temperature drop that causes tension in the membrane. This can be removed as the loading progresses and the solution becomes stable under the loaded curvatures and stresses.

Physical bending One can use plate/shell elements rather than membrane elements to retain the small bending stiffness actually present in the structure.

Artificial bending Some codes allow enhancement of the plate/shell bending stiffness through a factor, either on material properties or on section properties (suggested by Schur[5].)

Fading artificial bending Codes such as NASTRAN allow material properties to change with a loading parameter such as temperature. One can change the properties during the loading process to enhance bending at the outset, and then gradually fade back to the physical bending stiffness, or remove it entirely.

Artificial springs One can add lateral stiffness in the form of discrete spring elements at the nodes. Sizing of these spring elements is important if they are to remain active during the full load cycle. The springs should be sized so as to be 1% (say) of the lateral stiffness of the membrane under the rated load. (Of course, the presence of such springs will alter the load-deflection path up to the point of interest.)

Fading artificial springs The artificial springs discussed immediately above could be reduced to zero stiffness through material or stiffness alteration before the design load was reached.

Artificial rotation constraint If beam/shell elements are used to represent the balloon membrane, the rotational degrees of freedom can be artificially constrained to be zero. This makes the deflection pattern conform to a "stairstep" pattern. This stabilizes some solutions, at the expense of an increase in stiffness. For high-altitude research balloons, this loss in accuracy is so small as to be undetectable. (This trick is the least physical of those discussed, and could lead to trouble in balloons with larger ratios of membrane thickness to Radius h/R, and should not be used for smaller scale problems such as test specimens. It also fails for elements that lock up.)

Artificially softened material The instability in the displacement solution is believed to be due to overshoot when the stiffness of the system is understated. If the material properties of the membrane element were made to soften dramatically after some amount of strain, then the overshoot would not cause such a catastrophic elastic rebound. This might be in the nature of an elastic modulus which would decrease substantially.

Artificial viscosity If the inflation of the balloon is modeled in a dynamic way, the overshoot of the solution at a load step could be retarded by the use of artificial damping in the structure (or fluid, if modeled). Fluid mechanics researchers have long included artificial (numerical) damping in fluid systems in techniques to soften discontinuities.

Load	Code	Element	Thermal Strain	Original Bending	Artificial Bending	Fading	Spring	Rot. Const.	Converge
Pressure (Point)	MSC/NASTRAN	QUAD4 (Membrane)	No	No	No	No	No	No	No
	MSC/NASTRAN	QUAD4 (Membrane)	Yes	No	No	No	No	No	Yes
	MSC/NASTRAN	QUAD4 (Plate)	No	Yes	No	No	No	No	No
	MSC/NASTRAN	QUAD4 (Plate)	No	Yes	No	No	No	Yes	No
	MSC/NASTRAN	QUAD4 (Plate)	No	Yes	Yes (f=50)	No	No	No	No
	MSC/NASTRAN	QUAD4 (Plate)	No	Yes	Yes (f=50)	No	No	Yes	Yes
	MSC/NASTRAN	QUAD4 (Membrane & Plate)	No	No	Yes (f=50,000)	Yes	No	No	No
	MSC/NASTRAN	QUAD4 (Membrane & Plate)	No	No	Yes (f=50,000)	Yes	No	Yes	Yes
	Marc	# 18 (Membrane)	No	No	No	No	No	-	No
	Marc	# 18 (Membrane)	No	No	No	No	Yes	-	No
	Marc	# 30[1)] (Membrane)	No	No	No	No	No	-	No
	Marc	# 50 (Plate)	No	Yes	No	No	No	No	Yes
	Marc	# 50 (Plate)	No	Yes	No	No	No	Yes	Yes
	Marc	# 75 (Shell)	No	Yes	No	No	No	No	No
	Marc	# 75 (Shell)	No	Yes	No	No	Yes	No	Yes
	Marc	# 75 (Shell)	No	Yes	No	No	No	Yes	No
	Abaqus	M3D4 (Membrane)	No	No	No	No	No	No	No
	Abaqus	S4R[2)] (Shell)	No	Yes	No	No	No	No	No
	Abaqus	S4R (Shell)	No	Yes	No	No	No	Yes	Yes

Table 1: Convergence comparison for different programs and techniques: Standard disk under uniform pressure and point load (equivalent in total value to the pressure).

Comment:
1) 8-node element.
2) 4 Node reduced integration, doubly curved shell with hourglass control.

Macroelements

Several researchers have attempted to create membrane finite elements that incorporate wrinkling effects. The common idea is that a compression field causes wrinkling at a specific angle and spacing (much as in the web of a tension- field beam). This behavior can be exploited, in principal, by building empirical information into the element so that a coarser mesh would suffice, and the length scale of wrinkling would not have to be "captured" by a fine mesh.

W. Schur proposed a tension field element in unpublished notes in 1991, wherein the underlying stress field would be empirically described as to angle and spacing of wrinkles. Some progress was made, but the project was not completed.

M. Tomlin and others modified the membrane elements in MARC (#3,#26,#53,#18,#30,#72) by a pair of user-defined subroutines. They searched for principal stresses within the element, transformed to principal stress directions and "zeroed out" any principal compressive stress. This takes the element out of action in the direction perpendicular to the tension direction. The method also eliminates the need to "capture" the fine scale of wrinkling by use of fine mesh. (One should represent every wrinkle cross-section with 8 nodes per wave.)

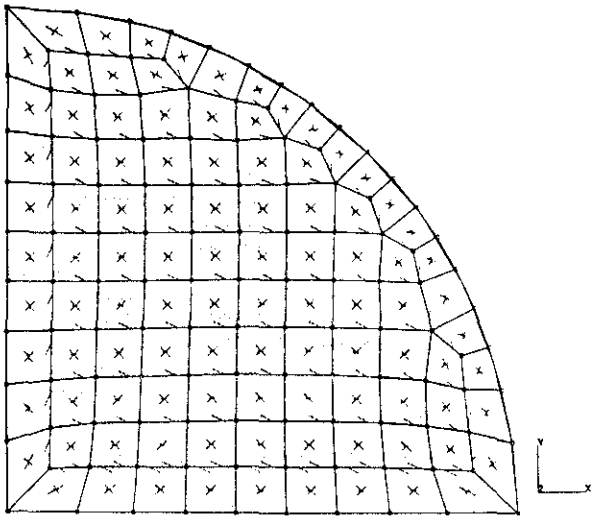

Figure 1: Mesh for a quarter disk solution

Numerical Analyses of a Flat, Initially Unstressed Disk Codes

Table 1 shows the results of many computer runs made for the standard 4 m disk problem (described above), using MSC/NASTRAN, ABAQUS and MARC. If the user uses conventional membrane modeling, (with no tricks from above) all runs fail on the first load step 10^{-8} MPa.

Surprisingly, the rotational constraint can be an effective way to get convergence (although the least motivated, physically). Other approaches are effective when carefully used.

The start-up problem has been found to be less severe in smaller specimens. As a result, a second study is presented to consider the scale effect between a polyethylene disk with 100 mm radius and the standard problem with 2000 mm radius (above). The study was done with the MARC #75 element, which is the most robust of the MARC surface elements for strong nonlinearities (Table 2).

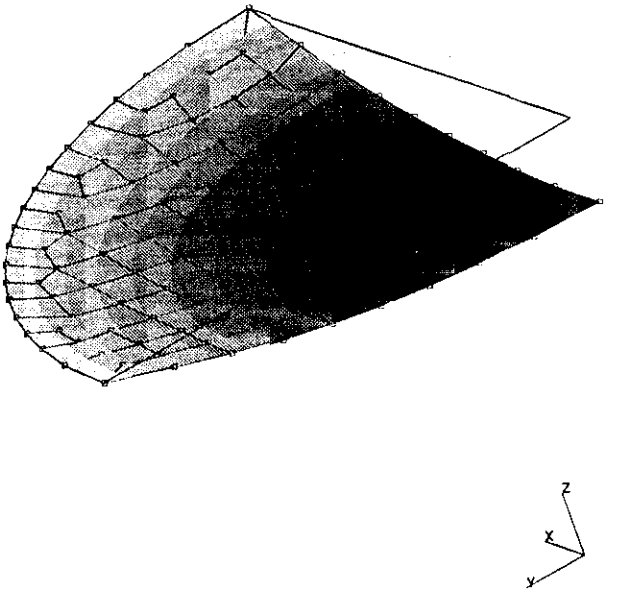

Figure 2: Deflection of disk under uniform pressure

Table 2: Effect of scale on convergence of flat membranes, MARC shell element #75

Radius (mm)	Constrain Rotations everywhere	Convergence
100	no	yes
100	yes	no
2000	no	no
2000	yes	no

This element appears to lock up when the trick of constraining rotations is used, and that trick is not advised for this element!

The problems with convergence of solution here seem to be due to the solution process rather than the element, per se. Much work needs to be done on solution techniques. At present, the solution of membrane inflation problems (especially with contact) is too difficult for standard practice.

Displacements are given for the center of the disk under distributed and concentrated center load in Fig 3, 4, and 5. There is excellent agreement between numerical and analytical solutions for the distributed load (pressure) in Fig 3. The point load, however, is a more severe case to model and a difference in codes is shown in Fig 4. Fig. 5 shows that a concentrated load, equivalent in total value to the distributed pressure, causes a greater deflection. No analytical solution is given.

Added mass calculation

If a solid body is immersed in a fluid and is then accelerated, pressures are generated which affect the fluid field to infinity. This creates kinetic energy in the fluid. One can define an effective mass of fluid accelerating with the body; this is called "added" mass. Historically, the calculation of added mass has been in the province of hydrodynamics.

Added masses are very important in studying dynamics of bodies which are submerged in relatively heavy fluids. Neutrally buoyant bodies such as balloons and submarines certainly qualify, as well as bodies which have large paddle-shaped surfaces which disturb the fluid, such as a thin disk oscillating normal to its surface.

Much recent progress in the area of numerical modeling of coupled acoustics/structures has been made. Several major software packages use boundary elements

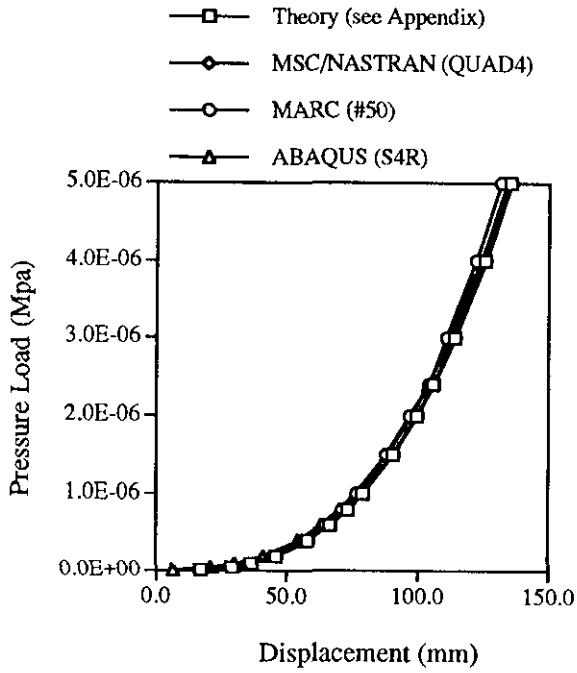

Figure 3: Comparison of displacements at center under pressure load by several codes

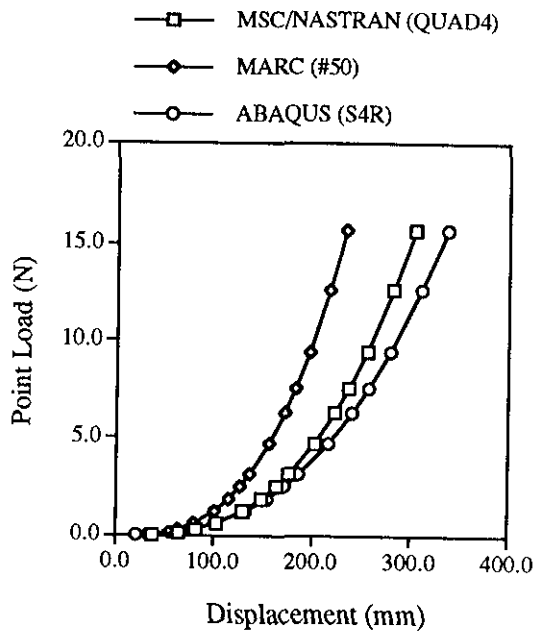

Figure 4: Comparison of displacements at center under point load by several codes

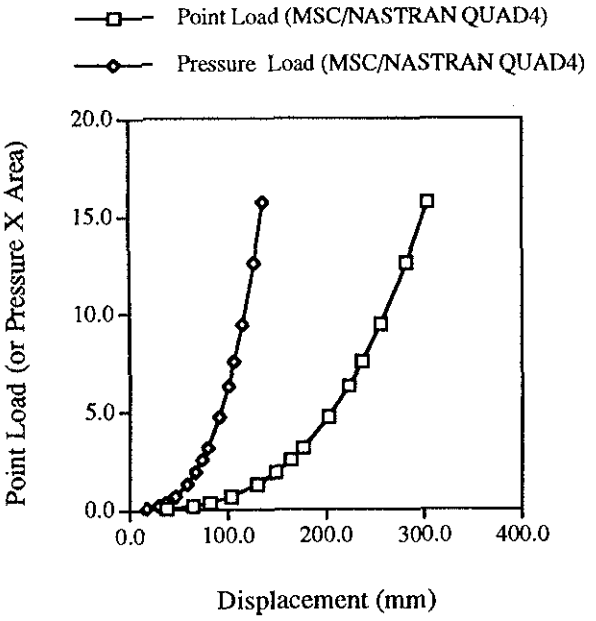

Figure 5: Comparison of displacements at center under pressure and point loads

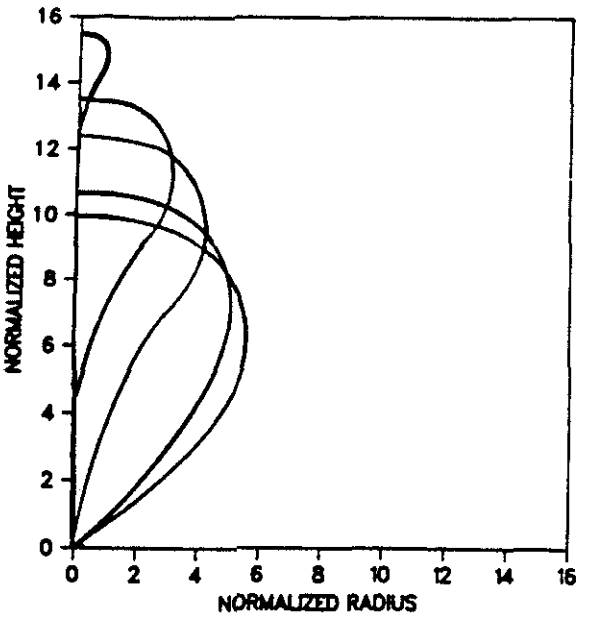

Figure 6: Cross-sections of balloons for varying inflation.[3]

for the fluid discretization. This modeling procedure can be used to determine the added mass due to rigid-body structural accelerations.[2] The effect of the pressure field is to retard the acceleration of the body, and the resulting added mass of the body can then be deduced. This capability has not existed before, and promises to aid the study of bodies such as balloons, parachutes and submarines where the bodies carry a large amount of fluid with them.

The acoustic field surrounding the balloon can be studied by using a pressure field solution and the boundary conditions cast into functions of pressure and velocity. The Helmholtz equation is solved:

$$\nabla^2 p + k^2 p = 0 \qquad (1)$$

with its appropriate boundary conditions.

A family of balloons of the Smalley type (zero circumferential stress) were studied by Anderson and Shah.[6] The balloon cross-sections are shown in Fig. 6. Inflation fractions of 0.0031 to 1.000 are used. Finite element meshes of three densities were used (Figs. 7, 8, 9). Results are given in Table 3. A volume correction had to be made to account for the fact that the elements composing the balloon shell are flat plates, and a faceted surface that results has less volume than a perfect sphere.

The balloon mesh was constructed by creating a 1/8 section of the balloon and then replicating it 8 times with the preprocessor I-DEAS. The completed model was faceted; no attempt was made to account for the scalloped nature of the segments as the film bulges from the load tapes.

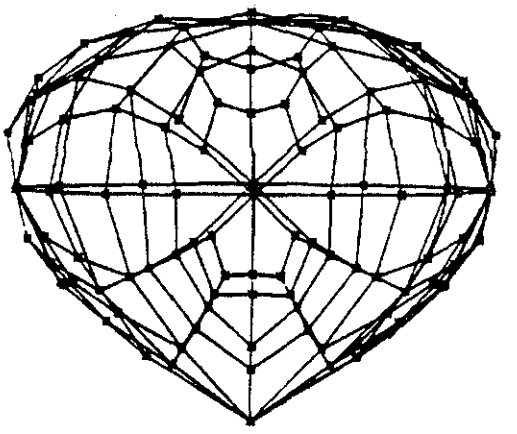

Figure 7: Coarse mesh for balloon at float.

The float results for added mass in the vertical (on-axis) and horizontal (lateral) directions are given in Table 3. The difference between the fine and the medium mesh is 2.8% and 0.5% for the axial and lateral cases, respectively. Perhaps the results are converging more slowly on axis because the balloon presents a "flatter"

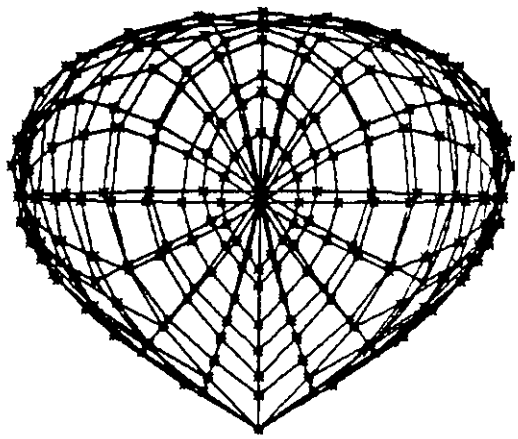

Figure 8: Medium mesh for balloon at float.

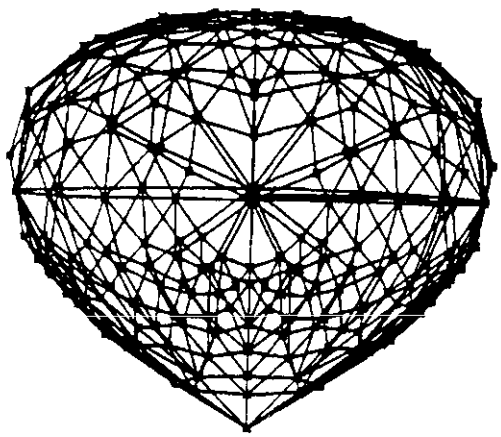

Figure 9: Fine mesh for balloon at float.

(more bluff) profile in that direction.

Convergence was from above, therefore the true values for added mass are slightly lower than the fine mesh result. For engineering purposes, the medium mesh is sufficient to study the partially-inflated family of balloons.

Table 3: Inertia coefficients for balloons at float

Mesh	Coarse	Medium	Fine
Elements	112	256	432
Nodes	114	226	218
Enclosed Volume	1.6416	1.7152	1.7262
Vertical Inertia	0.673	0.663	0.645
Horizontal Inertia	0.453	0.435	0.433
SYSNOISE CPU Time	6 sec	10 sec	16 sec

Results for a family of partially-inflated balloons are plotted in Fig. 10. The vertical (on-axis) inertia is higher than the horizontal (lateral). The inertial coefficients ranged from 0.42 to 0.64, depending on the inflation and the orientation of acceleration.

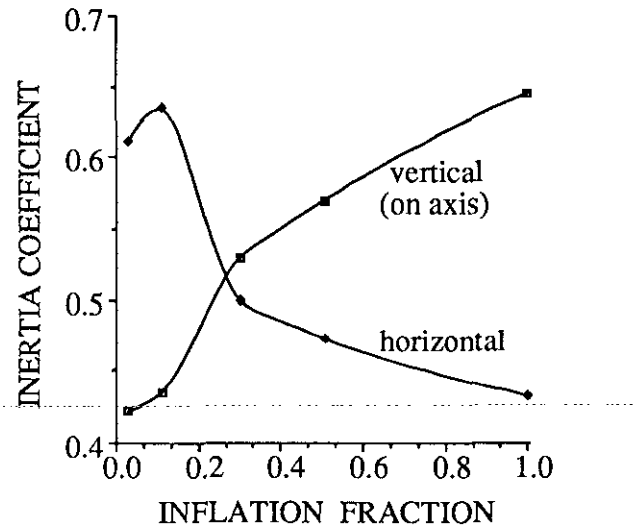

Figure 10: Added mass for high-altitude balloon.

An analytical expression was found for the added mass as a function of inflation fraction. The best fit for vertical added mass was a cubic, as shown in Fig. 11:

$$y(x) = 0.39967 + 0.47881x - 0.30341x^2 + 0.069664x^3$$

The best fit for horizontal added mass is a quadratic,

shown in Fig. 12.

$$y(x) = 0.64944 - 0.50739x + 0.29101x^2$$

The erratic nature of the coefficients at small inflation fractions was due to the difficulty in defining the small bubble at the end of a long "rope" of collapsed polyethylene film. The volume of the "rope" has been neglected in these calculations. The values for added mass at small inflation fractions should be viewed as having less precision.

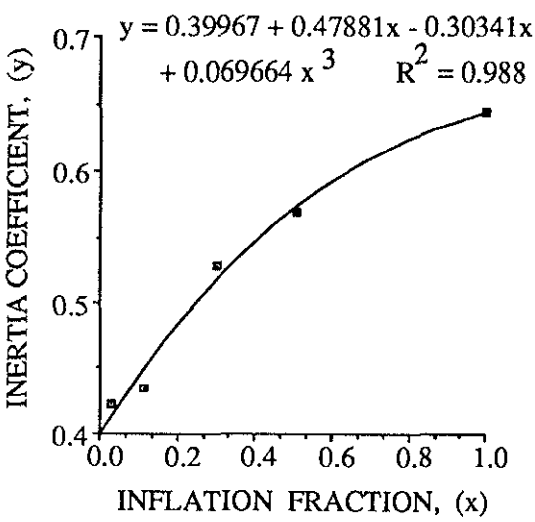

Figure 11: Cubic fit to vertical added mass for balloon.

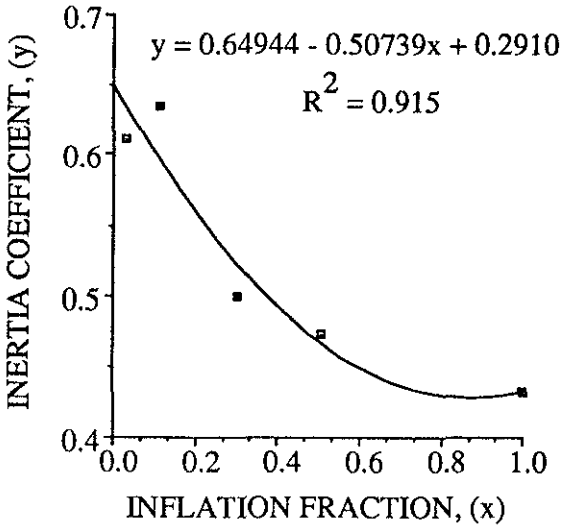

Figure 12: Quadratic fit to horizontal added mass for balloon.

There has been little experimental data to compare with this theory. The NASA/GSFC Wallops Flight Facility has flown tethered small-scale balloons and has measured inertia coefficients for vertical acceleration of approximately 0.55.[4] In the past, researchers often applied the value of 0.5 for spheres to the study of high-altitude balloon. The current values will allow added mass to be adjusted continuously with flight conditions (fraction of inflation). Although there limited experimental data at present to confirm the theoretical predictions for added mass, there is agreement in the dynamics community that the infinitesimal theory for added mass is on the same firm foundation as infinitesimal theory of elasticity, so no surprises are expected.

Thermal analysis

As a balloon comes from behind the earth's shadow and is heated by the sun, convective currents appear inside the balloon. The polyethylene sheet will absorb more energy from the sun than the helium, and will be relatively warm. The helium inside the balloon will rise at the outer diameter and subside down the center core.

To model this buoyant convection problem requires that the program account for density changes due to heating. Several commercial codes (FIDAP, STAR-CD nd CENTRIC) are able to handle this problem. Others (e.g. RAMPANT) cannot at present handle the thermal expansion of gas due to heat addition, in their incompressible solutions. RAMPANT could, in principal handle this as a compressible problem, but doesn't converge well at Mach numbers below 0.1.

The code STAR-CD was used in an axisymmetric model of the balloon heating problem. A 22 million cubic foot high-altitude, zero-pressure balloon is modeled as a sphere intersecting with a cone, with a 5 ft diameter disk open to the atmosphere at the bottom. Conditions are taken at standard 36,000 m altitude (120,000 ft) where the temperature is 250 degrees Kelvin. It is assumed that the entire polyethylene skin is subjected to a heat influx of 10 watts/meter^2. The flux is ramped up from 0 watts/m^2 at time zero to 10 watts/m^2 at two seconds, and maintained at 10 watts/m^2 thereafter. The open throat at the bottom is assumed to stay at atmospheric pressure, and at 250 degrees K.

The properties of helium at 36,000 m were taken to be: specific heat at constant pressure = 5,240 J/kg °K; thermal conductivity = 0.1338 W/°K m; and viscosity = 28.53 $\times 10^{-6}$ kg/m sec.

Figure 13 shows the axisymmetric mesh used. A velocity field at time 12 seconds is shown in Fig. 14, where the length of the arrow denotes the velocity magnitude. The figure is difficult to read, but shows upflow

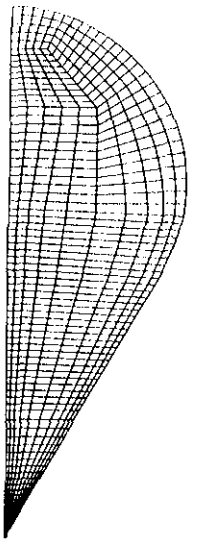

Figure 13: Mesh for axisymmetric study of buoyant convection

at the outer diameter and downflow in the interior. The maximum velocity 2.20 m/sec. Of course, the convection pattern is axisymmetric; all convective cells are ring-like.

Such numerical studies of the buoyant convection problem ought to help clear up the large temperature differences observed in practice. The lift of the balloon will depend, as a function of time, on the effects of the heating rate. Also, one could determine whether the mixing tends to spill helium through the open throat. Three dimensional studies will be possible.

Concluding Remarks

The analysis of inflatable membrane structures is still in its infancy. Problems in solution convergence occur due to the starting problem of unstressed membranes, and due to wrinkling during the inflation process. It is important in the next year to develop standard models to judge FEA program performance. There may be suitable "tricks" for taming the divergent nature of the solution, particularly in simpler problems. The general wrinkling problem with many contact possibilities seems unlikely to yield in the near future, although progress can be made in simpler geometries where insight helps the analyst.

The inertia coefficients obtained for high-altitude balloons should help in developing flight simulation codes that model dynamic balloon behavior. Common

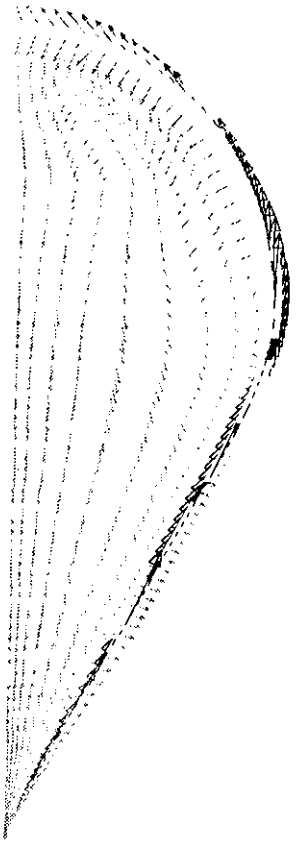

Figure 14: Velocity field in balloon

sources of excitation include ballast drops which cause axial acceleration and side winds that cause lateral accelerations. The inertia coefficients obtained range from 0.43 to 0.64 depending on inflation and direction of acceleration. These new values should now replace the classical value of 0.5 for a sphere, which has been used in many earlier calculations.

The convection field inside the heated balloon can now be studied by CFD codes, such as STAR-CD. Other codes will be able to handle the low-speed, buoyant convection in the near future. It is hoped that full 3-D simulation will show the presence of closed convective cells in the balloon, and show the temperature field within the balloon. Experiments to date lead one to believe that there are substantial temperature gradients maintained by such cells.

Acknowledgments

The authors are grateful for numerical computations with STAR-CD that were made by Dr. Kurichi Kumar of Automated Analysis Corporation.

The computer software used in this paper was made available through University programs from MARC Analysis Research Corporation (MARC), Numerical Integration Technologies (SYSNOISE), Structural Dynamics Research Corp. (I-DEAS), and The MacNeal-Schwendler Corp. (MSC/NASTRAN). The use of these programs is greatly appreciated.

References

[1] Kraus, H., "Thin Elastic Shells", John Wiley, Inc., New York, 1967, pp. 85-86.

[2] SYSNOISE Theoretical Manual, Version 4.3, Numerical Integration Technology, Heverlee, Belgium, July, 1990.

[3] Rand, J., "Shape and Stress of an Ascending Balloon," Winzen International, Inc., San Antonio TX, Report No. WII-9936-FR-01, June, 1987.

[4] Robbins, E., and Martone, M., "Determination of Balloon Gas Mass and Revised Estimates of Drag and Virtual Mass Coefficients," COSPAR XXVII Plenary Meeting and Associated Activities, The Hague, The Netherlands, July 1990.

[5] Schur, W., "Recent Advances in the Structural Analysis of Scientific Balloons" COSPAR XXVII Plenary Meeting and Associated Activities, Paper P.3-M.1.02, The Hague, The Netherlands, July 1990.

[6] Anderson, W.J. and Shah, G.N., "Added Mass of High-Altitude Balloons", AIAA International Balloon Technology Conference, Paper 91-3693, Albuquerque, Oct., 1991.

Appendix

Strain-Displacement Relations for a Circular Flat Membrane

It is assumed that 1) the circular flat membrane has nonlinear strain-displacement relations, 2) a pressure load q is applied on the membrane. Because this problem is axisymmetric, the displacements of the membrane can be described by two components such as radial u and vertical w components. The strain in the radial direction is:

$$\epsilon_r = \frac{du}{dr} + \frac{1}{2}(\frac{dw}{dr})^2 \tag{2}$$

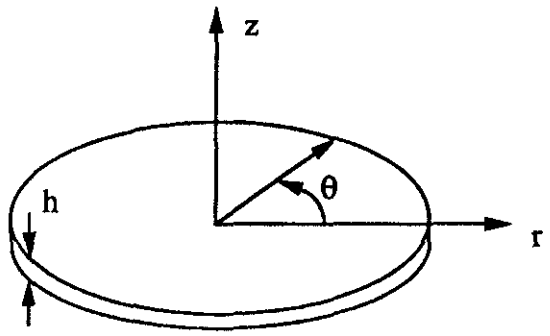

Figure 15: Circular flat membrane

The strain in the tangential direction is:

$$\epsilon_t = \frac{2\pi(r+u) - 2\pi r}{2\pi r} = \frac{u}{r} \tag{3}$$

Eq. 2 can be rewritten by using Eq. 3:

$$\epsilon_r = \epsilon_t + r\frac{d\epsilon_t}{dr} + \frac{1}{2}(\frac{dw}{dr})^2 \tag{4}$$

From Hooke's law, the strains can be written by membrane forces per unit lenth N_r and N_t:

$$\epsilon_r = \frac{1}{Eh}(N_r - \nu N_t) \tag{5}$$

$$\epsilon_t = \frac{1}{Eh}(N_t - \nu N_r) \tag{6}$$

The radial displacement u can be rewritten by Eq. 3 and 6.

$$u = \frac{r}{Eh}(N_t - \nu N_r) \tag{7}$$

From equations 4, 5 and 6, the relation between membrane forces is derived:

$$\frac{1}{Eh}[(N_r - N_t - r\frac{dN_t}{dr}) + \nu(N_r - N_t + r\frac{dN_r}{dr})] - \frac{1}{2}(\frac{dw}{dr})^2 = 0 \tag{8}$$

Equilibrium Equation

The equilibrium equation in the radial direction is:

$$N_r - N_t + r\frac{dN_r}{dr} = 0 \tag{9}$$

A useful relation in the vertical direction can be obtained by force equilibrium in Fig. 17.

$$2\pi N_r \frac{dw}{dr} - \pi r^2 q = 0 \tag{10}$$

It becomes

$$N_r \frac{dw}{dr} = r\frac{q}{2} \tag{11}$$

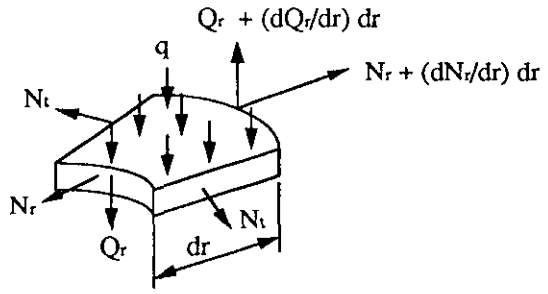

Figure 16: Membrane force in an infinitesimal element of a membrane

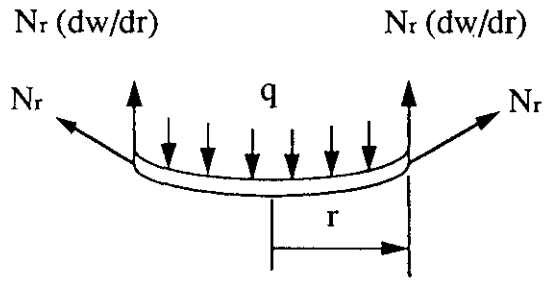

Figure 17: Infinitesimal element of a membrane under pressure

Substitution of Eq. 9 into Eq. 8 becomes

$$r\frac{d}{dr}(N_r + N_t) + \frac{Eh}{2}(\frac{dw}{dr})^2 = 0 \qquad (12)$$

The three equations 9, 11 and 12 contain three unknown functions N_r, N_t and w. For the new description of the three equations, dimensionless parameters are defined.

$$p = \frac{q}{E}, \xi = \frac{r}{h}, S_r = \frac{N_r}{Eh}, S_t = \frac{N_t}{Eh} \qquad (13)$$

From the dimensionless parameters, the three equations become:

$$\frac{d}{d\xi}(\xi S_r) - S_t = 0 \qquad (14)$$

$$S_r\frac{dw}{hd\xi} - \frac{p}{2}\xi = 0 \qquad (15)$$

$$\xi\frac{d}{d\xi}(S_r + S_t) + \frac{1}{2}(\frac{dw}{hd\xi})^2 = 0 \qquad (16)$$

Boundary Conditions

A circular flat membrane is clamped on the circular boundary. The boundary conditions are described for radial displacement u (Eq. 7) and vertical displacement w.

$$(u)_{\xi=a/h} = h\xi(S_t - \nu S_r)_{\xi=a/h} = 0 \qquad (17)$$

$$(w)_{\xi=a/h} = 0 \qquad (18)$$

Approximate Solution by Power Series

The functions S_r and $\frac{dw}{hdr}$ are represented by the power series of ξ.

$$S_r = \sum_{n=0}^{\infty} B_n\xi^n \qquad (19)$$

$$\frac{dw}{hd\xi} = \sum_{n=0}^{\infty} C_n\xi^n \qquad (20)$$

where B_n and C_n are constants to be determined later.

From equations 15, 19 and 20, constants C_n can be expressed in terms of B_n:

$$\begin{aligned} C_0 &= 0 \\ C_1 &= \frac{p}{2B_0} \\ C_k &= -\frac{1}{B_0}\sum_{m=1}^{k-1} B_m C_{k-m} \qquad k = 2,3,4 \end{aligned} \qquad (21)$$

Substitution of Eq. 19 into Eq. 14 gives

$$S_t = \sum_{n=0}^{\infty}(n+1)B_n\xi^n \qquad (22)$$

Relations for B_n are obtained from equations 16, 19, 20 and 22.

$$\begin{aligned} B_1 &= 0 \\ B_m &= -\frac{1}{2m(m+2)}\sum_{k=1}^{m-1} C_k C_{k-1} \\ &(m = 2,\ 3,\ 4\ ..) \end{aligned} \qquad (23)$$

In numerical calculation, physical properties (radius a, Young's modulus E, Poisson's ratio ν and pressure q) are given. The constant B_0 is determined to satisfy the boundary condition (Eq. 17). Consecutively, all the other constants, S_r and $\frac{dw}{hd\xi}$ can be obtained. From the $\frac{dw}{hd\xi}$ and boundary condition (Eq. 18), the vertical displacement w of the circular flat membrane can be obtained.